UNIVERSITY OF
BATH

University of Bath

Label-Free Impedimetric Aptasensor with Antifouling Surface Chemistry:

a Prostate Specific Antigen Case Study

Pawan Jolly[a], Nello Formisano[a], Ján Tkáč[b], Peter Kasák[c], Christopher G. Frost[d],

Pedro Estrela[a,*]

[a] Department of Electronic & Electrical Engineering, University of Bath, Bath BA2 7AY, United

Kingdom; Email: P.Jolly@bath.ac.uk, N.Formisano@bath.ac.uk, P.Estrela@bath.ac.uk

[b] Department of Glycobiotechnology, Institute of Chemistry, Slovak Academy of Sciences, Dúbravská

cesta 9, 845 38 Bratislava, Slovakia; Email: Jan.Tkac@savba.sk

[c] Center for Advanced Materials, Qatar University, P.O. Box 2713, Doha, Qatar; Email:

Peter.Kasak@qu.edu.qa

[d] Department of Chemistry, University of Bath, Bath BA2 7AY, United Kingdom; Email:

C.G.Frost@bath.ac.uk

[*] Corresponding author: Department of Electronic & Electrical Engineering, University of Bath,

Claverton Down, Bath BA2 7AY, United Kingdom

E-mail: P.Estrela@bath.ac.uk

Phone: +44-1225-386324

Abstract

We here report the development of an aptamer based biosensor for the investigation of prostate specific antigen (PSA), a biomarker found in blood for prostate cancer (PCa), using electrochemical impedance spectroscopy (EIS). The study concentrates on a clinical application where a specific and sensitive label-free detection could be performed in real blood samples using EIS. Two types of PSA aptasensor were fabricated by immobilizing (i) a self-assembled monolayer comprising of 6-mercaptohexanol (MCH) and thiolated-DNA aptamer and (ii) 11-mercaptoundecanoic acid for covalent immobilization of amine terminated DNA aptamers and sulfo-betaine terminated thiol as an antifouling agent on a polycrystalline gold surface. Upon incubation of PSA with the DNA aptamer-based biosensor a decrease of charge transfer resistance (R_{ct}) was observed due to the partial screening of the DNA aptamer charge by PSA. Thiol terminated sulfo-betaine based sensors can detect PSA levels lower than 1 ng/ml. Validation of the aptasensor is provided by surface plasmon resonance measurements. Sulfo-betaine moiety also prevents any significant non-specific binding of the control protein human serum albumin (HSA) as compared to high non-specific binding with MCH-based sensors. A debate is presented on the effect of the measurement buffer on the values and the direction of R_{ct} changes on the aptasensors and the need to cautiously select suitable measurement conditions in order to obtain reliable results. This is the first report to date where a DNA aptamer-based biosensor was developed using thiol-terminated sulfo-betaine, which is a simple surface chemistry for the development of promising, cost-effective, label-free and sensitive electrochemical detection platforms for a range of analytes.

Keywords: DNA aptamers; prostate specific antigen; electrochemical impedance spectroscopy; antifouling properties

1. Introduction

One of the biggest challenges in the field of cancer detection is its early diagnosis before it metastases to other organs. Detection of biomarkers – i.e. biochemical blueprints of a certain disease that can be found in altered levels in blood, urine, tissue and saliva – could be used as a method for early diagnosis of the disease, leading to more successful treatments [1,2]. Among cancer concerning men worldwide, prostate cancer (PCa) makes its mark as one of the leading causes of cancer related morbidity among men over 50 years of age [3]. PCa can be very lethal, as it lacks any symptoms in its early stage and is incurable if diagnosed in its later stages [4]. The most frequently used biomarker in blood to detect and monitor patients with PCa is prostate specific antigen (PSA). It is a 30-34 kDa single chain glycoprotein primarily produced by the prostate epithelium [5]. The altered level of PSA above the cut-off value of 4 ng/ml in blood is often suspected to be linked with PCa [6,7]. However, increased PSA levels in blood can also be found in patients with benign prostate conditions, which can give rise to misdiagnosis. Even though PSA is no longer considered to be a very reliable PCa biomarker, there is a general consensus that it is an important marker that needs to be included in any panel of biomarkers to be detected for PCa diagnosis.

A range of PSA detection methods have been developed, which employ the use of expensive antibodies due to their high selectivity to the antigen [8-12]. However, these methods bear high cost, *in vivo* antibody production and laborious experiments. One of the alternatives to antibodies is to employ aptamers. Aptamers are single stranded DNA or RNA strands that can be screened using the *in vitro* chemical process SELEX (systematic evolution of ligands by exponential enrichment) [13-15]. Once developed, aptamers can then be easily synthesized and commercially purchased. Not only aptamers can bind to their target while undergoing a conformational change with strong affinity and specificity, they can also keep most of their functionality even after multiple regeneration steps [16]. They can also be easily modified with a variety of functional groups expanding their use in different applications [17]. Aptamers have gained significant importance in the past decade and have been integrated with electrochemical techniques to detect proteins, whole cells, drugs and various other molecules [18-22]. Electrochemical biosensors have always been in the spotlight for research since

they require simple instrumentation and their ease to use, low cost, high sensitivity, rapid and robust nature. There is a substantial number of reports in the literature on impedimetric aptasensors exploiting the conformational change properties of the aptamers along with other factors that change the impedance of the system [23-29]. PSA-specific DNA aptamer-based biosensors that have been reported so far, employ the use of gold nanoparticles (AuNPs) for signal enhancement. One of the two methods is based on optical detection for PSA aptamer conjugated with AuNPs [30]. Another is an electrochemical-based sensor where the surface chemistry reported uses a complex layer-by-layer development and using bovine serum albumin for blocking the surface to reduce non-specific binding [31].

Surface modification plays a vital factor in biosensor development since it affects both sensitivity and selectivity. Typically, bioreceptor molecules are immobilised on gold electrode surfaces using self-assembled monolayers (SAMs) in order to make the bioreceptor available for interaction and passivate the electrode to reduce non-specific interactions. One of the most accepted approaches to achieve this goal is by alkanethiol chemistry. Alkanethiols can be easily adsorbed and form a SAM [32] on a clean gold surface through gold-sulphur bonds. It is been reported that longer alkane chains give a more compact structure with minimal defects [33]. An important consideration is whether a modified electrode surface prevents non-specific binding so that it could be used for real clinical samples. Among various gold electrode surface modifications, 6-mercaptohexanol (MCH) has been widely used as a spacer molecule with enough evidence on the efficiency of the DNA biosensor signal output which is dependent on the spacing between the probes on the gold surface [34,35] or detection of PSA using aptamers [36]. A thiol-terminated sulfo-betaine spacer molecule has been reported for surface modification to develop lectin-based biosensors with enhanced antifouling properties [37]. However, to date, the use of thiol-terminated sulfo-betaine to develop aptamer-based biosensors has not been reported.

In this study, a simple and potentially sensitive electrochemical aptamer-based biosensor is proposed using thiol-terminated sulfo-betaine as an antifouling surface chemistry. A 32 bases long DNA aptamer for PSA [38] has been used for as a case study. The study also reports for the first time the

use of electrochemical impedance spectroscopy (EIS) as a detection technique for PSA dose response using aptamers. The results are validated by means of surface plasmon resonance (SPR) data. Although a previous report employed EIS to perform interfacial surface characterization of a PSA aptamer-based biosensor [31], it has not been used as a technique to monitor PSA levels on aptasensors. The current study also compares MCH and thiol terminated sulfo-betaine for their effect on the sensitivity and selectivity of the fabricated impedimetric biosensors. We report the effect of different buffers on EIS signal change and present a debate on buffer influence on the measurement data, applicable to most EIS-based aptasensors. The PSA aptamer based electrochemical biosensor is a prospective platform for clinical applications with acceptable precision and repeatability.

2. Materials and Methods

2.1. Reagents

PSA aptamers (thiolated PSA aptamer, 5'-HS-$(CH_2)_6$-TTT TTA ATT AAA GCT CGC CAT CAA ATA GCT TT-3' and amine terminated PSA aptamer, 5'-NH_2-(CH2)$_6$- TTT TTA ATT AAA GCT CGC CAT CAA ATA GCT TT -3') were synthesized by Sigma-Aldrich (Gillingham, UK). Prostate–specific antigen was obtained from Merck Chemicals Ltd (Beeston, UK). Human serum albumin (HSA), 11-mercaptoundecanoic acid (MUA), 6-mercapto-1-hexanol (MCH), trisma base, potassium phosphate monobasic solution (1 M), potassium phosphate dibasic solution (1 M), potassium sulphate, potassium hexacyanoferrate (III), potassium hexacyanoferrate (II) trihydrate, ethylenediaminetetraacetic acid (EDTA, 0.5 M), N-hydroxysuccinimide (NHS), N-(3-dimethylaminopropyl)-N′-ethylcarbodiimide hydrochloride (EDC), ethanolamine, Tween 20, hexaammineruthenium (III) chloride and magnesium chloride were all purchased from Sigma-Aldrich. Human glandular kallikrein 2 (hK2) was obtained from R&D Systems (Abingdon, UK). Thiol terminated sulfo-betaine ((R)-3-((2-(5-(1,2-dithiolan-3-yl)pentanamido)ethyl)dimethylammonio)propane-1-sulfonate) was synthesized according to a previously published procedure [35]. All other reagents were of analytical grade. All aqueous

solutions were prepared using 18.2 MΩ cm ultra-pure water with a Pyrogard filter (Millipore, Feltham, UK).

2.2. Apparatus

The electrochemical measurements were performed using a μAUTOLAB III / FRA2 potentiostat (Metrohm Autolab, Utrecht, The Netherlands) using a three-electrode cell setup with a Hg/Hg_2SO_4 (K_2SO_4) reference electrode (BASi, West Lafayette, IN, USA) connected *via* a salt bridge filled with 0.1 M phosphate buffer (PB) containing 0.1 M KCl (pH 7.4) and a Pt counter electrode (ALS, Tokyo, Japan). The impedance spectrum was measured in 0.1 M PB measurement buffer with 0.1 M KCl containing 10 mM of the ferro/ferricyanide $[Fe(CN)_6]^{3-/4-}$ redox couple (hexacyanoferrate II/III) in a frequency range from 100 kHz to 100 mHz, with a 10 mV a.c. voltage superimposed on a bias d.c. voltage of -0.190 V *vs.* Hg/Hg_2SO_4 (corresponding to the formal potential of the redox couple).

Surface plasmon resonance (SPR) experiments were carried out in a dual-channel SPR7000DC from Reichert Technologies (Depew, NY, USA). Gold coated SPR sensors were immobilised in situ with the aptamer and measurements carried out in 10 mM PBS with 0.05% Tween 20 under flow conditions. The flow rate was kept constant at 25 µl/min upon injection of different protein concentrations, allowing 10 minutes for binding followed by 5 minutes for dissociation of unbound protein

2.3. Sample preparation

Gold disk working electrodes with a radius of 1.0 mm (CH Instruments, Austin, TX, USA) were cleaned using a protocol based on that reported by Keighley *et al.* [32]: electrodes were mechanically polished for 2 min with 1 µm diamond solution (Buehler, Lake Bluff, IL, USA) and thereafter for 5 min with 50 nm alumina slurry (Buehler) on respective polishing pads (Buehler). In between each step 10 min sonication and rinsing in ultra-pure water was practiced in order to remove any remaining particles. Electrodes were then electrochemically cleaned in 0.5 M H_2SO_4 by scanning the potential

between the oxidation and reduction of gold, −0.05 V and +1.1 V *versus* a Hg/Hg$_2$SO$_4$ reference electrode, for 50 cycles until no further changes in the voltammogram were noticed. Finally, electrodes were washed with ultra-pure water.

For the fabrication of PSA aptasensor with MCH, clean gold electrodes were exposed to 150 µl of mixed thiolated DNA aptamer/MCH immobilization solution for 16 h in a humidity chamber. A high concentration of MCH was prepared in ethanol which was diluted to working concentration in binding buffer and measurement buffer respectively. Prior to addition of MCH, DNA aptamers were heated to 95°C for 10 min followed by gradual cooling over 30 min to room temperature. After immobilization, electrodes were rinsed with DI water to remove unattached DNA aptamers. In order to ensure complete thiol coverage of the gold surface, the electrodes were thereafter backfilled with 1 mM MCH for 1 h. Electrodes were then rinsed with ultra-pure water and placed in the measurement buffer for 1 h to stabilize the SAM. An optimized 1% DNA aptamer mole fraction to total thiol was used to fabricate the biosensor [36].

For the fabrication of PSA aptasensors with sulfo-betaine, clean gold electrodes were immersed in a 1:99 ratio of two thiols, MUA:thiol terminated sulfo-betaine and incubated for 16 h. Stock solution of MUA was prepared in pure ethanol and stored at -20°C until use and thiol terminated sulfo-betaine was stored dry at the same temperature and prepared fresh before use in distilled water. Amine terminated DNA aptamers were immobilized using standard amine coupling reaction with the carboxylic groups of MUA that were activated by 0.2 M EDC and 0.05 M NHS. The electrodes were incubated in a mixture of EDC/NHS for 20 min followed by incubation with 1 µM amine terminated DNA aptamer solution in the binding buffer for 2 h leading to covalent immobilization of aptamers on the activated SAM. Later, the SAM was washed with DI and incubated in 1 M ethanolamine (pH 8.5) for 30 min to block all the un-reacted activated sites of MUA. Finally, the electrodes were rinsed with DI water and placed in the measurement buffer for stabilization for 1 h. The same immobilisation procedure was used for the SPR gold electrodes.

For binding studies, different concentrations of PSA were prepared in the binding buffer. 100 µM HSA was also prepared in the binding buffer for checking for non-specific interactions. The

specificity of the aptamer was checked by studying its interaction with different concentrations of hk2 in the same buffer.

3. Results and Discussion

Impedimetric aptasensors were fabricated with sulfo-betaine (see structure in Figure 1c) as a spacer molecule for better anti-fouling properties (Figure 1a). For comparison, aptasensors using a standard MCH spacer were also studied (Figure 1b).
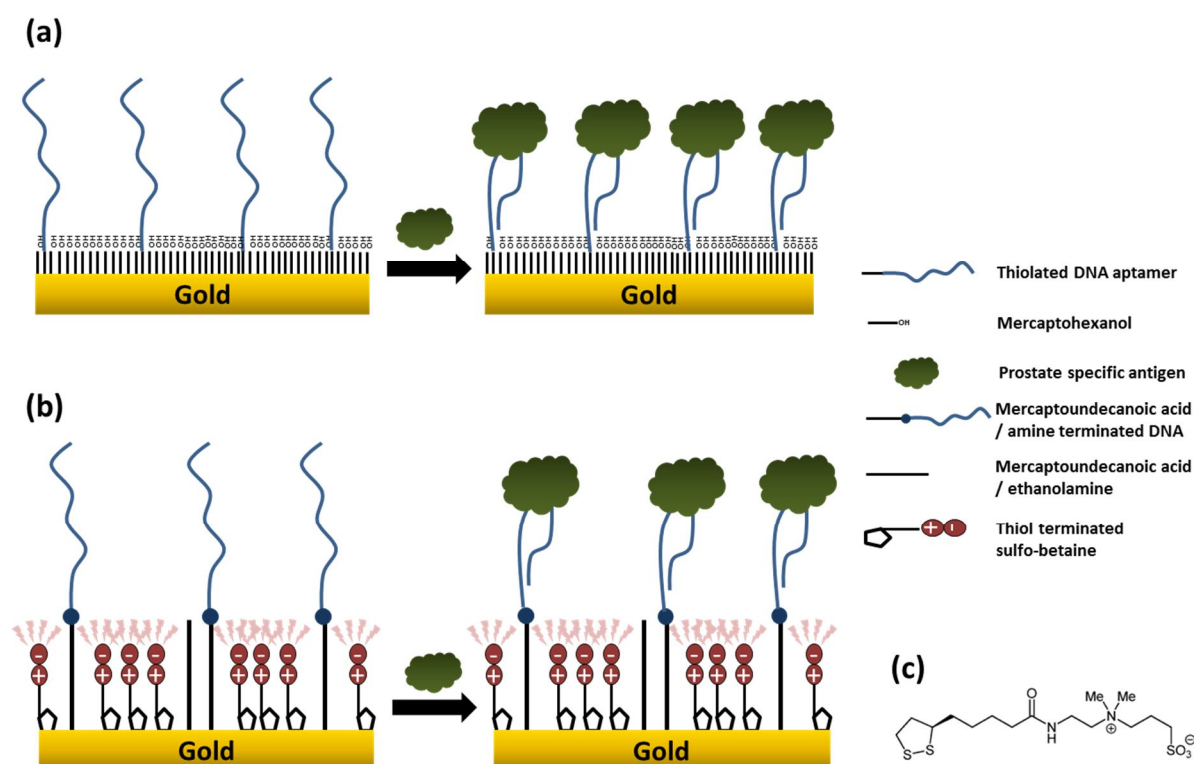

Figure 1: SAMs with DNA aptamers on a gold surface before and after incubation with PSA.
a) thiolated aptamer with MCH; b) amine terminated aptamer with sulfo-betaine; c) structure of the thiol-modified sulfo-betaine.

3.1. Electrochemical characterization of thiol terminated DNA aptamers with MCH

Co-immobilization of thiol modified DNA aptamer and MCH onto gold electrodes was used to fabricate functional electrodes for PSA detection. A typical Nyquist plot for the system is shown in Figure 2a. The charge transfer resistance (R_{ct}) of the SAM prepared was determined by fitting the

spectra to a Randles equivalent circuit, with a constant phase element (non-ideal capacitance), in parallel with the charge transfer resistance (R_{ct}) and a Warburg element (W) that models diffusion. After aptamer immobilisation, R_{ct} values of around $60 \, \Omega \, cm^2$ are observed. Upon incubation with PSA, a reduction in R_{ct} was observed indicating binding with DNA aptamers. In the example shown in Figure 2, R_{ct} decreased by 15% upon interaction with 10 µg/ml of PSA. This decrease is contradictory to what has been reported in the literature for PSA where an increase of R_{ct} has been observed [31], even though these studies used EIS mainly to characterize the bio-recognition layer and not for dose response determination. A reduction of R_{ct} upon aptamer-analyte interaction has also been reported for a different aptasensor using a lysozyme aptamer, where the reduction in charge transfer resistance upon binding of lysozyme to its specific DNA aptamer was attributed to screening of DNA charges by the lysozyme [39].
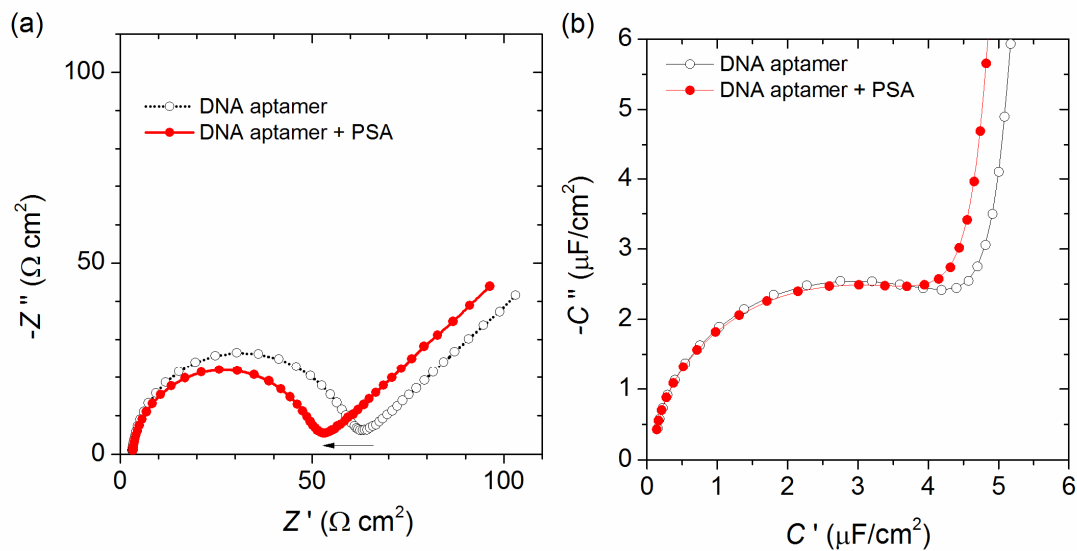

Figure 2: Typical EIS characteristics for DNA aptamer/MCH functionalized gold electrodes in 10 mM ferro/ferricyanide $[Fe(CN)_6]^{3-/4-}$ in 0.1 M phosphate buffer (PB) solution containing 0.1 M KCl (pH 7.4). a) Nyquist impedance plot; b) Cole-Cole complex capacitance plots at high frequencies. Reduction in R_{ct} was recorded on binding of PSA with DNA aptamer in binding buffer for 30 min. The PSA concentration was 10 µg/ml.

The reduction of charge transfer resistance could arise from two reasons. Firstly, upon binding, PSA might screen the charges of the DNA aptamer. Secondly, as PSA is also a charged protein, it could be

that more positive charges are exposed because of the protein architecture itself. Consequently, as there is screening of charges of DNA, there is a reduction on the electrostatic barrier to the ferro/ferricyanide anions towards the electrode surface, leading to lowering of the R_{ct} value of the system.

In order to evaluate the capacitance of the system, a complex capacitance was defined as:

$$C^* = C' + j\,C'' \equiv \frac{1}{j\omega Z} = \frac{-Z''}{j\omega |Z|^2} + j\frac{-Z'}{j\omega |Z|^2} \tag{1}$$

and calculated from the impedance data. Figure 2b shows the Cole-Cole capacitance plot at high frequencies before and after PSA interaction. A semi-circle is observed indicating a fast capacitive process, followed by a larger semi-circle due to an ultra-slow process [40], which is typical of impedance-based sensors using redox markers in solution [41]. No significant changes in the capacitance are observed upon PSA interaction; however the onset of the second semicircle appears at lower C' values, which could be associated with an increase of conductive paths in the SAM/biolayer [42]. Considering that the impedance of the system is dominated by the electrostatic potential barrier of the DNA layer towards the negatively charged redox marker, the increase of conductive paths could be associated with a reduction on the net charge of the biolayer and, therefore, consistent with the hypothesis of DNA charge screening by PSA.

3.2. Electrochemical characterization of amine terminated DNA aptamers with sulfo-betaine

Electrodes fabricated with amine terminated DNA aptamers immobilized on a mixed SAM consisting of MUA with thiol terminated sulfo-betaine *via* conventional EDC/NHS coupling agents through amino link were characterized with the EIS technique. These functionalized electrodes were used to detect PSA. The EIS characteristics recorded for different PSA concentrations are presented in Figure 3. Two semicircles are observed in the Nyquist impedance plot: a small semicircle at high frequencies, presumably due to relaxation effects of the SAM [41], followed by a large one at lower frequencies. The impedance of the system was fitted by using two *RC* circuits in series. The resistance of the first semicircle remains constant (with variations lower than 5%) throughout the experiments

10

with resistance values in the order of $250\,\Omega\,cm^2$, while the capacitance (Figure 3b), with initial values of $15\,\mu F/cm^2$, shows a negligible increase for concentrations up to 25 ng/ml, after which it increases linearly with log[PSA] until it saturates at a value of $\Delta C/C \approx 8\%$ for 1000 ng/ml PSA. The larger semicircle at lower frequencies is best described with a constant phase element in parallel with the charge transfer resistance (R_{ct}) of the system. Again, a negative signal change in R_{ct} was recorded upon binding with PSA: R_{ct} decreases from $8.9\,k\Omega\,cm^2$ after aptamer immobilisation, down to $5.3\,k\Omega\,cm^2$ at the highest PSA concentration used. The low frequency capacitance remains constant within 1% at a value of $90\,\mu F/cm^2$. The fact that sulfo-betaine is considerably longer than MCH explains why the charge transfer resistance values are significantly larger for the sulfo-betaine aptasensors.
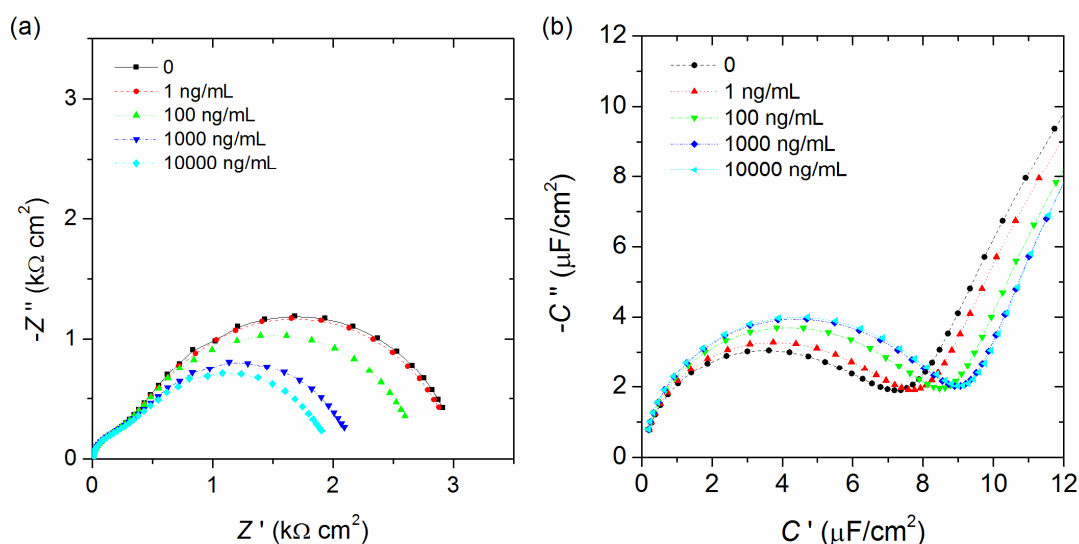

Figure 3: Typical EIS characteristics for amine terminated aptamer functionalized gold electrodes with sulfo-betaine for different concentrations of PSA in 10 mM ferro/ferricyanide $[Fe(CN)_6]^{3-/4-}$ in 0.1 M phosphate buffer (PB) solution containing 0.1 M KCl (pH 7.4).

A dose response curve of R_{ct} with different concentrations of PSA relative to blank measurements is shown in the inset of Figure 4. The binding curve follows a Freundlich-type of equation ($\Delta R_{ct}/R_{ct} \propto [PSA]^n$) until 1000 ng/ml, after which it slowly tends to saturation. With this configuration the sensitivity was increased and it was possible to detect PSA concentrations lower than 1 ng/ml.

However, the signal change recorded was relatively very small. The reason for such a small signal change could be the net effect of different processes happening at the molecular level. The first dominating event happening is the change in the conformation of DNA aptamers on binding with PSA which should result in an increase in R_{ct}. However, our assumption is at such a low concentration of DNA aptamer, it is very likely that all the aptamers are already in their stable conformation leading to exclusion of the effect of conformational changes on R_{ct}. In addition, there is the screening of negative charges of DNA aptamers upon binding with PSA resulting into reduction in R_{ct}. Lastly, there is an increase in R_{ct} because of binding of PSA molecules resulting into a further passivation of the electrode, which can hinder the access of the redox probes to a close distance of the electrode. The charges of protein also add on to R_{ct} values, which may be creating more positive charge closer to the surface. Consequently, the net R_{ct} of the system depends on the combination of all the factors.
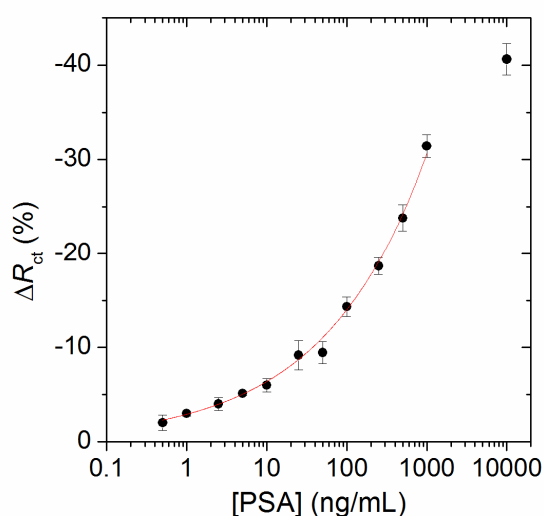

Figure 4: Charge transfer resistance dose response for amine terminated aptamer electrodes with with sulfo-betaine for different PSA concentrations in 0.1 M PB (pH 7.4) containing 10 mM [Fe(CN)$_6$]$^{3-/4-}$ and 0.1 M KCl. Incubation of functionalized sensors with PSA was for 30 min. The error bars represent the standard deviation obtained for six samples. The line corresponds is a fit of the data to a Freundlich equation and serves as a guide to the eye.

A high standard deviation was also observed at each sample point. Such a sample-to-sample variation could be a result of differences in the initial R_{ct} values of each electrode, due to variations in the

number of DNA aptamers immobilized on the surface. Although for the study 1% MUA mole fraction to total thiol [MUA+thiol terminated sulfo-betaine] was used to prepare the first SAM layer, it should be noted that the final concentration of DNA aptamers will be less than 1% depending on the efficiency of covalent coupling *via* EDC/NHS. It is assumed that because of the different diffusion rates of MUA and sulfo-betaine as well as the added flexibility of the sulfo-betaine chain, the surface ratio will be different than the solution ratio. Adding to this, the efficiency of EDC/NHS coupling reaction also plays a vital role. As a consequence, there is a significant difference in the initial R_{ct} values for different samples prepared in the same way (average value 8.95 kΩ cm^2 with a standard deviation of 4.28 kΩ cm^2). The actual variations in R_{ct} upon PSA binding, on the other hand, are quite reproducible.

The binding of the aptamer with PSA was validated by means of SPR data. Using the same surface immobilisation process as for the sulfo-betaine impedimetric aptasensors, the SPR signal was monitored upon injection of different concentrations of PSA. Figure 5 shows the SPR equilibrium response for each PSA concentration. A typical hyperbolic dose response is observed: $y = y_{max} + c/(K_d+c)$ where c is the concentration and K_d the affinity constant. Fitting the data yields an affinity constant of $K_d = 9.50 \pm 0.47$ ng/ml.
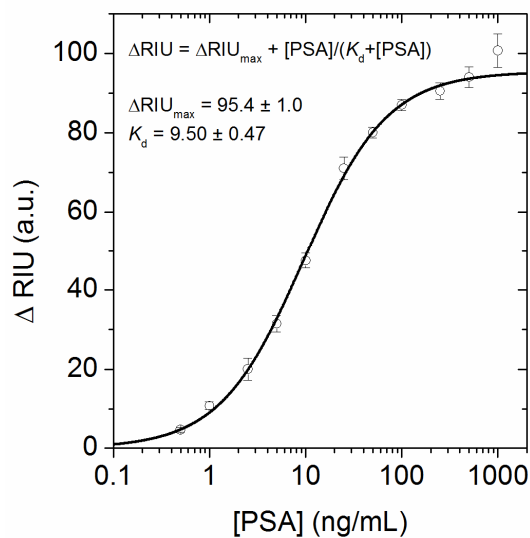

Figure 5: Variation in the equilibrium SPR signals with respect to the baseline for different concentrations of PSA. Measurements were carried out in 10 mM PBS with 0.05% Tween 20. The

line is a fit of the data to a hyperbolic dose response equation. The error bars represent the standard deviation obtained for three samples.

3.3. Investigation of antifouling properties and specificity of fabricated sensors

Another key point of consideration is the antifouling efficiency of the fabricated aptasensor for its application with real blood samples. The antifouling efficiency depends on the quality and composition of the SAM. Human serum albumin (HSA) was used as a control protein to study non-specific binding as it is one of the major constituents of human blood. Upon incubation with 100 µM HSA (*circa* 67 µg/ml), the thiol aptamer/MCH sensor showed an increase of 12.5% in the R_{ct} value. Given the decrease observed with target PSA, this non-specific interaction can be distinguished from a true positive. However, in a more complex medium like blood this could lead to decreased sensitivity. Electrodes with thiol terminated sulfo-betaine surface chemistry were also studied for non-specific adsorption. These electrodes showed a negligible change in R_{ct} (<1%), indicating good anti-fouling properties. SPR measurements with 100 µM HSA confirmed the low non-specific signal: an SPR signal of $\Delta RIU = 6$ was observed, which is similar to the signal observed for the lowest concentration of PSA tested (0.5 ng/ml).

The specificity of the aptasensors with thiol terminated sulfo-betaine was checked by incubating freshly prepared sensors with hK2. Both PSA and hK2 are kallikrein proteins sharing 70% homology. Upon incubation with 10 ng/ml and 100 ng/ml of hK2, R_{ct} decreases by -1.1% and -1.6%, respectively. For comparison, decreases of -6.0% and -14.3% were observed for similar concentrations of PSA. These results indicate that not only the sulfo-betaine moiety effectively prevents non-specific interactions, but the aptamer is also highly selective towards PSA.

3.4. Effect of changing buffers on stability of SAM

Another important point to take into consideration for EIS-based aptasensors is the stability of SAM in different buffers. It is often reported in the literature that the binding of proteins to aptamers is

performed in a different buffer from the measurement buffer. Hence, we investigated if the change in R_{ct} values of the fabricated sensor was due to the binding of protein and not because of buffer effects. Both types of fabricated PSA aptasensors were used for this study. These samples were firstly stabilised in 0.1 M PB (pH 7.4) containing 0.1 M KCl and then measurements taken in 0.1 M PB (pH 7.4) containing 10 mM $[Fe(CN)_6]^{3-/4-}$ and 0.1 M KCl. Figure 6 shows the time that electrodes can take to give stable R_{ct} values without addition of any protein. It should be noted that the stabilisation time profile depends on the surface chemistry and buffers used. The total time for stabilisation of the sensor can be minimised by careful sensor design and storage conditions. However, the results here presented highlight the need to always check for the stabilisation of the impedance signals prior to test an interaction.
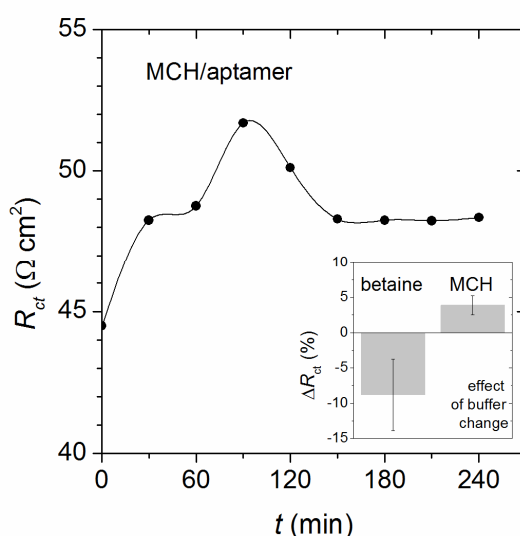

Figure 6: Change in charge transfer resistance (R_{ct}) of an electrode measured in 30 min intervals in 0.1 M PB (pH 7.4) containing 10 mM $[Fe(CN)_6]^{3-/4-}$ and 0.1 M KCl. The inset shows the effect of introducing a 10 mM Tris-HCl (pH 7.4) buffer containing 10 mM KCl, 10 mM MgCl2 and 0.05% Tween 20 for 30 min without any PSA in both sulfo-betaine/aptamer and MCH/aptamer sensors. Measurements were carried out in 0.1 M PB (pH 7.4) containing 10 mM $[Fe(CN)_6]^{3-/4-}$ and 0.1 M KCl. The error bars represent the standard deviation obtained for four samples.

Once a stable R_{ct} has been recorded, the electrodes were then immersed in 10 mM Tris-HCl (pH 7.4) containing 10 mM KCl, 10 mM $MgCl_2$ and 0.05% Tween 20 for 30 min without any PSA. The EIS

measurement was again recorded and the results are represented in the inset of Figure 6. It can be clearly seen that regardless of surface chemistry used, the buffer itself can cause instability of the SAM which is reflected by a change in R_{ct}. It is possible that the positive R_{ct} variation observed by Liu *et al.* [31] is in fact due to the change in buffers during PSA incubation and not due to binding of PSA. Hence, it is very important to maintain the same buffer conditions throughout the EIS measurement in order to obtain reliable data.

4. Conclusions

With the aim to improve diagnosis of prostate cancer, this study reports a development of a PSA aptasensor with antifouling chemistry to detect the biomarker in complex samples. The main focus of this report was to investigate the use of aptamers as a possible replacement to antibodies – a study which can be expanded to other PCa biomarkers. Moreover, incorporation of other molecules like MCH or sulfo-betaine enables optimization of the sensor surface for better detection and preventing non-specific binding. Different surface chemistries were investigated for their performance in the detection of PSA.

This work reports a decrease in R_{ct} upon binding of PSA to DNA aptamer. This shift is probably due to the screening of the charges on DNA aptamers. This work also reports for the first time the use of sulfo-betaine with DNA aptamers. Although the optimization of surface density was a challenge, the fabricated aptasensors could potentially be used to detect PSA levels lower than 1 ng/ml, which falls in the clinically relevant range (1-10 ng/ml). With the MCH based PSA aptasensor the lowest concentration of PSA that could be detected was 10 µg/ml.

Both the PSA aptasensor fabrication processes, i.e. with MCH and sulfo-betaine, were compared for their capability to prevent fouling. It was observed that PSA aptasensors with MCH surface chemistry gave a very high non-specific binding with human serum albumin, whereas PSA aptasensor with sulfo-betaine surface modification showed negligible signal. Sulfo-betaine moiety can therefore be used as a promising feature to construct biosensors for clinical applications.

16

Furthermore, a discussion on the effects of buffer was presented. It was demonstrated for the first time until date that by changing the buffer conditions during the EIS measurements, instabilities of the SAM could take place, which can therein result in changes in R_{ct} regardless of having the analyte in the solution. The study showed how important it is to perform stability tests of the fabricated aptasensors in order to obtain reliable data.

Acknowledgements

References

[1] B.K. Edwards, M.L. Brown, P.A. Wingo, H.L. Howe, E. Ward, L.A. Ries, D. Schrag, P.M. Jamison, A. Jemal, X.C. Wu, C. Friedman, L. Harlan, J. Warren, R.N. Anderson, L.W. Pickle, Annual report to the nation on the status of cancer, 1975-2002, featuring population-based trends in cancer treatment, *J. Natl. Cancer Inst.* 97 (2005) 1407-1427.

[2] J.A. Ludwig, J.N. Weinstein, Biomarkers in cancer staging, prognosis and treatment selection, *Nat. Rev. Cancer* 5 (2005) 845-856.

[3] A.W. Partin, M.W. Kattan, E.N. Subong, P.C. Walsh, K.J. Wojno, J.E. Oesterling, P.T. Scardino, J.D. Pearson, Combination of prostate-specific antigen, clinical stage, and gleason score to predict pathological stage of localized prostate cancer: a multi-institutional update, *J. Am. Med. Assoc.* 277 (1997) 1445-1451.

[4] V.M. Velonas, H.H. Woo, C.G. Remedios, S.J. Assinder, Current status of biomarkers for prostate cancer, *Int. J. Mol. Sci.* 14 (2013) 11034-11060. doi: 10.3390/ijms140611034

[5] S. Gilgunn, P.J. Conroy, R. Saldova, P.M. Rudd, R.J. O'Kennedy, Aberrant PSA glycosylation – a sweet predictor of prostate cancer, *Nat. Rev. Urol.* 10 (2013) 99-107. doi: 10.1038/nrurol.2012.258

[6] W.J. Catalona, D.S. Smith, T.L. Ratliff, K.M. Dodds, D.E. Coplen, J.J. Yuan, J.A. Petros, G.L. Andriole, Measurement of prostate-specific antigen in serum as a screening test for prostate cancer, *New Engl. J. Med.* 324 (1991) 1156-1161.

[7] D.A. Healy, C.J. Hayes, P. Leonard, L. McKenna, R. O'Kennedy, Biosensor developments: application to prostate-specific antigen detection, *Trends Biotechnol.* 25 (2007) 125-131.

[8] Y. Seto, T. Iba, K. Abe, Development of ultra-high sensitivity bioluminescent enzyme immunoassay for prostate-specific antigen (PSA) using firefly luciferase, *Luminescence* 16 (2001) 285-290.

[9] B. Acevedo, Y. Perera, M. Ruiz, G. Rojas, J. Benítez, M. Ayala, J. Gavilondo, Development and validation of a quantitative ELISA for the measurement of PSA concentration, *Clin. Chim. Acta* 317 (2002) 55-63.

[10] K.W. Wee, G.Y. Kang, J. Park, J.Y. Kang, D.S. Yoon, J.H. Park, T.S. Kim, Novel electrical detection of label-free disease marker proteins using piezoresistive self-sensing micro-cantilevers, *Biosens. Bioelectron.* 20 (2005) 1932-1938.

[11] J. Okuno, K. Maehashi, K. Kerman, Y. Takamura, K. Matsumoto, E. Tamiya, Label-free immunosensor for prostate-specific antigen based on single-walled carbon nanotube array-modified microelectrodes, *Biosens. Bioelectron.* 22 (2007) 2377-2381.

[12] N.V. Panini, G.A. Messina, E. Salinas, H. Fernández, J. Raba, Integrated microfluidic systems with an immunosensor modified with carbon nanotubes for detection of prostate specific antigen (PSA) in human serum samples, *Biosens. Bioelectron.* 23 (2008) 1145-1151.

[13] T. Hermann, D.J. Patel, Adaptive recognition by nucleic acid aptamers, *Science* 287 (2000) 820-825.

[14] S. Song, L. Wang, J. Li, C. Fan, J. Zhao, Aptamer-based biosensors, *Trends Anal. Chem.* 27 (2008) 108-117. doi: 10.1016/j.trac.2007.12.004

[15] M. Mascini, I. Palchetti, S. Tombelli, Nucleic acid and peptide aptamers: fundamentals and bioanalytical aspects, *Angew. Chem. Int. Ed.* 51 (2012) 1316-1332. doi: 10.1002/anie.201006630

[16] J.H. Lee, M.V. Yigit, D. Mazumdar, Y. Lu, Molecular diagnostic and drug delivery agents based on aptamer-nanomaterial conjugates, *Adv. Drug Deliv. Rev.* 62 (2010) 592-605. doi: 10.1016/j.addr.2010.03.003

[17] L. Sheng, J. Ren, Y. Miao, J. Wang, E. Wang, PVP-coated graphene oxide for selective determination of ochratoxin A via quenching fluorescence of free aptamer, *Biosens. Bioelectron.* 26 (2011) 3494-3499. doi: 10.1016/j.bios.2011.01.032

[18] Y. Du, C. Chen, J. Yin, B. Li, M. Zhou, S. Dong, E. Wang, Solid-state probe based electrochemical aptasensor for cocaine: a potentially convenient, sensitive, repeatable, and integrated sensing platform for drugs, *Anal. Chem.* 82 (2010) 1556-1563. doi: 10.1021/ac902566u

[19] H. Kuang, W. Chen, D. Xu, L. Xu, Y. Zhu, L. Liu, H. Chu, C. Peng, C. Xu, S. Zhu, Fabricated aptamer-based electrochemical "signal-off" sensor of ochratoxin A, *Biosens. Bioelectron.* 26 (2010) 710-716. doi: 10.1016/j.bios.2010.06.058

[20] C. Sun, X. Liu, K. Feng, J. Jiang, G. Shen, R. Yu, An aptazyme-based electrochemical biosensor for the detection of adenosine, *Anal. Chim. Acta* 669 (2010) 87-93. doi: 10.1016/j.aca.2010.04.057

[21] L. Feng, Y. Chen, J. Ren, X. Qu, A graphene functionalized electrochemical aptasensor for selective label-free detection of cancer cells, *Biomaterials* 32 (2011) 2930-2937. doi: 10.1016/j.biomaterials.2011.01.002

[22] L. Bai, R. Yuan, Y. Chai, Y. Zhuo, Y. Yuan, Y. Wang, Simultaneous electrochemical detection of multiple analytes based on dual signal amplification of single-walled carbon nanotubes and multi-labeled graphene sheets, *Biomaterials* 33 (2012) 1090-1096. doi: 10.1016/j.biomaterials.2011.10.012

[23] A.E. Radi, J.L. Acero Sánchez, E. Baldrich, C.K. O'Sullivan, Reusable impedimetric aptasensor, *Anal. Chem.* 77 (2005) 6320-6323.

[24] C. Deng, J. Chen, Z. Nie, M. Wang, X. Chu, X. Chen, X. Xiao, C. Lei, S. Yao, Impedimetric aptasensor with femtomolar sensitivity based on the enlargement of surface-charged gold nanoparticles, *Anal. Chem.* 81 (2008) 739-745. doi: 10.1021/ac800958a

[25] B. Li, Y. Wang, H. Wei, S. Dong, Amplified electrochemical aptasensor taking AuNPs based sandwich sensing platform as a model, *Biosens. Bioelectron.* 23 (2008) 965-970.

[26] T. Hianik, J. Wang, Electrochemical aptasensors–recent achievements and perspectives, *Electroanalysis* 21 (2009) 1223-1235. doi: 10.1002/elan.200904566

[27] A. Sassolas, L.J. Blum, B.D. Leca-Bouvier, Electrochemical aptasensors, *Electroanalysis* 21 (2009) 1237-1250. doi: 10.1002/elan.200804554

[28] A.H. Loo, A. Bonanni, M. Pumera, Impedimetric thrombin aptasensor based on chemically modified graphenes, *Nanoscale* 4 (2012) 143-147. doi: 10.1039/c1nr10966a

[29] F. Rohrbach, H. Karadeniz, A. Erdem, M. Famulok, G. Mayer, Label-free impedimetric aptasensor for lysozyme detection based on carbon nanotube-modified screen-printed electrodes, *Anal. Biochem.* 421(2), 454-459. doi: 10.1016/j.ab.2011.11.034

[30] Z. Chen, Y. Lei, X. Chen, Z. Wang, J. Liu, An aptamer based resonance light scattering assay of prostate specific antigen, *Biosens. Bioelectron.* 36 (2012) 35-40. doi: 10.1016/j.bios.2012.03.041

[31] B. Liu, L. Lu, E. Hua, S. Jiang, G. Xie, Detection of the human prostate-specific antigen using an aptasensor with gold nanoparticles encapsulated by graphitized mesoporous carbon, *Microchim. Acta* 178 (2012) 163-170. doi: 10.1007/s00604-012-0822-5

[32] S.D. Keighley, P. Li, P. Estrela, P. Migliorato, Optimization of DNA immobilization on gold electrodes for label-free detection by electrochemical impedance spectroscopy, *Biosens. Bioelectron.* 23 (2008) 1291-1297. doi: 10.1016/j.bios.2007.11.012

[33] S.D. Keighley, P. Estrela, P. Li, P. Migliorato, Optimization of label-free DNA detection with electrochemical impedance spectroscopy using PNA probes, *Biosens. Bioelectron.* 24 (2008) 906-911. doi: 10.1016/j.bios.2008.07.041

[34] N. Formisano, P. Jolly, M. Cromhout, R. Fogel, J.L. Limson, P. Estrela, Correlating electrochemical impedance spectroscopy and quartz crystal microbalance with dissipation signals for optimisation of aptamer-based biosensors, *Submitted for publication.*

[35] T. Bertok, L. Klukova, A. Sediva, P. Kasák, V. Semak, M. Micusik, M. Omastova, L. Chovanová, M. Vlček, R. Imrich, A. Vikartovska, J. Tkac, Ultrasensitive impedimetric lectin biosensors with efficient antifouling properties applied in glycoprofiling of human serum samples, *Anal. Chem.* 85 (2013) 7324-7332. doi: 10.1021/ac401281t

[36] N. Savory, K. Abe, K. Sode, K. Ikebukuro, Selection of DNA aptamer against prostate specific antigen using a genetic algorithm and application to sensing, *Biosens. Bioelectron.* 26 (2010) 1386-1391. doi: 10.1016/j.bios.2010.07.057

[37] J.C. Love, L.A. Estroff, J.K. Kriebel, R.G. Nuzzo, G.M. Whitesides, Self-assembled monolayers of thiolates on metals as a form of nanotechnology, *Chem. Rev.* 105 (2005) 1103-1170.

[38] S. Campuzano, M. Pedrero, C. Montemayor, E. Fatás, J.M. Pingarrón, Characterization of alkanethiol-self-assembled monolayers-modified gold electrodes by electrochemical impedance spectroscopy, *J. Electroanal. Chem.* 586 (2006) 112-121. doi: 10.1016/j.jelechem.2005.09.007

[39] M.C. Rodriguez, A.N. Kawde, J. Wang, Aptamer biosensor for label-free impedance spectroscopy detection of proteins based on recognition-induced switching of the surface charge, *Chem. Commun.* (2005) 4267-4269.

[40] B. Roling, M. Drüschler, B. Huber, Slow and fast capacitive process taking place at the ionic liquid/electrode interface, *Faraday Discuss.* 154 (2012) 303-311. doi: 10.1039/c1fd00088h

[41] F.C.B. Fernandes, A. Santos, D.C. Martins, M.S. Góes, P.R. Bueno, Comparing label free electrochemical impedimetric and capacitive biosensing architectures, *Biosens. Bioelectron.* 57 (2014) 96-102. doi: 10.1016/j.bios.2014.01.044

[42] G. Valincius, T. Meškauskas, F. Ivanauskas, Electrochemical impedance spectroscopy of tethered bilayer membranes, *Langmuir* 28 (2012) 977-990. doi: 10.1021/la204054g